

Establishment and characterization of a novel, spontaneously immortalized retinoblastoma cell line with adherent growth

JEONG HUN KIM¹, JIN HYOUNG KIM², YOUNG SUK YU^{1,5},
DONG HUN KIM³, CHONG JAI KIM⁴ and KYU-WON KIM²

¹Department of Ophthalmology, Seoul National University College of Medicine and Seoul Artificial Eye Center, Clinical Research Institute, Seoul National University Hospital; ²NeuroVascular Coordination Research Center, College of Pharmacy and Research Institute of Pharmaceutical Sciences, Seoul National University, Seoul; ³Department of Radiology, College of Medicine, Chosun University, Gwangju; ⁴Department of Pathology, Seoul National University College of Medicine, Seoul, Korea

Received April 10, 2007; Accepted June 11, 2007

Abstract. Retinoblastoma is the most common intraocular cancer of childhood, however, only a few cultured retinoblastoma cell lines are available to date. In the present study, we established a new human retinoblastoma cell line with adherent growth, named SNUOT-Rb1. The SNUOT-Rb1 cell line was established from an eye with retinoblastoma, which was enucleated from a 3-year-old Korean child. SNUOT-Rb1 has morphological and biochemical characteristics common to previous human retinoblastoma cell line, Y79: morphological features of fibroblast- or ganglion-like cells, and biochemical features of expression of glial fibrillary acidic protein and neuron-specific enolase. However, compared to Y79, SNUOT-Rb1 has a unique characteristic of growing in adherence, and the doubling time of SNUOT-Rb1 is shorter than Y79 in adherent or floating growth. In analysis of the tumorigenic potential of SNUOT-Rb1 in nude mice, orthotopic implantation of SNUOT-Rb1 mimics the pattern of local growth of retinoblastoma. In comparative genomic hybridization analysis, we found that SNUOT-Rb1 has significant chromosomal imbalances on chromosome 3, 9, 10, 11, 14, 16, 17, and 22. Therefore, SNUOT-Rb1 could be useful in studying the biological and genetic characteristics of retinoblastoma for insights into the heredity and genetics of childhood cancer.

Introduction

Retinoblastoma is the most common intraocular cancer of childhood with an incidence of approximately 1 in 15,000 to 20,000 births, which represents the prototypic model for

inherited cancers (1-3). *RBI* was the first tumor-suppressor gene to be identified, leading to the discovery of a whole new class of antioncogenes and greatly contributing to advances in the management of solid tumors in children.

Mutations in both alleles of the *RBI* gene, a tumor suppressor in 13q14, are causative of the development of retinoblastoma (4). Additional mutations, however, may be prerequisite for *Rb1*^{-/-} cells to progress to tumorigenesis (5). Also, a study of *Rb1* knock-out mice showed that loss of both alleles of the *Rb1* gene is insufficient for tumor formation (6). In 60% of all retinoblastoma, the tumor is restricted to one eye and the *Rb1* gene mutations are somatic and non-hereditary, whereas 40% are germ-line and hereditary (7).

The study of the molecular mechanisms of oncogenesis in retinoblastoma has led to an understanding of the role that tumor suppressors, oncogenes, and deoxyribonucleic acid (DNA) repair genes play in development of the disease. For research on cancer biology, tumor cell culture is an effective tool to identify the cell of origin as well as subsequent genetic defects that contribute to pathogenesis. The majority of *in vitro* and *in vivo* investigations for retinoblastoma have been carried out using human retinoblastoma cell lines such as Y79 (8) and WERI-Rb1 (9), which both spontaneously grow in suspension. Here we report the establishment and characterization of a new, spontaneously immortalized human retinoblastoma cell line, designated SNUOT-Rb1. SNUOT-Rb1, naturally growing in attachment, demonstrates some features common to, or different from other retinoblastoma cell lines. This newly established cell line, SNUOT-Rb1, can be an *in vitro* model to provide the means for the study of characterizing properties of human retinoblastoma.

Materials and methods

Establishment of the tumor cell line. The sample was provided with informed consent, institutional review board approval was obtained, and the tenets of the Declaration of Helsinki were followed. Primary tumor material was obtained from eyes and immediately transferred into RPMI-1640 without FBS. The tissue was minced, washed with PBS to remove

Correspondence to: Dr Young Suk Yu, Department of Ophthalmology, College of Medicine, Seoul National University, Seoul 110-744, Korea
E-mail: ysyu@snu.ac.kr

Key words: retinoblastoma cell line, adherent growth, orthotopic implantation, comparative genomic hybridization

any residual blood. The washed cells were then cultured in RPMI-1640 containing penicillin-streptomycin (10 ml/l, Gibco BRL, Invitrogen, Carlsbad, CA) and 10% fetal bovine serum (Gibco BRL) at 37°C in 5% CO₂ in a humidified incubator. The culture medium was changed every three days. Cultured tumor cells were observed daily under a phase-contrast microscope.

Induction differentiation of SNUOT-Rb1. All-*trans* retinoic acid (RA; Sigma-Aldrich, St. Louis, MO) was dissolved in dimethylsulphoxide (DMSO; Sigma) as a stock solution at 10 mM. After 2 days in culture, the medium was replaced with fresh medium containing 10 μM RA or 0.1% DMSO (negative control). Cultures were examined over 10 days. Culture medium was changed every three days.

Reverse transcription-polymerase chain reaction (RT-PCR). Total RNA was prepared from cells using TRIzol reagent, according to the manufacturer's protocol (Invitrogen, New Zealand). RNA was dissolved in diethyl pytocarbonate (DEPC)-H₂O and first-strand cDNA synthesis was performed using SuperScript™ II RNase H-reverse transcriptase (Invitrogen) and an oligo-dT primer. The cDNA was subjected to 30 cycles of amplification using the primers; RARα forward 5'-CCTCTACCCCGCATCTACAA-3' and reverse 5'-TTGAGGAGGGTGATCTGGTC-3', GAPDH forward 5'-AAGGT CATCCCTGAGCTGAA-3' and reverse 5'-CCCCTCTTCAAGGGGTCTAC-3' at 95°C for 1 min, 58°C for 1 min, and 72°C for 1 min. The PCR products were analyzed on 1% agarose gels stained with ethidium bromide.

Immunocytochemistry of Y79 cells and SNUOT-Rb1. Cells were grown as attachment cultures, seeded at a concentration of 1x10⁵ cells/ml, on coverslips (Deckglaser, Germany) pre-coated with 0.1 mg/ml poly-D-lysine (Sigma) and incubated at 37°C for one day. Coverslips were blocked for 30 min with DakoCytomation Protein Block (DakoCytomation, USA) at room temperature, and then incubated with anti-human glial fibrillary acidic protein (GFAP) (1:100, DakoCytomation) or anti-human neuron-specific enolase (NSE) (1:50, DakoCytomation) antibodies at -4°C overnight. For negative control, mouse IgG was used as the primary antibody. Then, cells were incubated at room temperature for 60 min with polyclonal goat anti-mouse immunoglobulin (1:5,000, DakoCytomation). Finally, samples were detected with an AEC substrate kit (Zymed Lab. Inc. South San Francisco, USA).

Rate of cell growth study. The growth curve of the tumor cells was obtained by seeding the cells at 2x10⁴ cells/well in a 12-well plate (Nunc, Roskilde, Denmark). The media were changed every two days. The number of cells per well was counted every day for 8 days after incubation at 37°C in 5% CO₂ of a humidified incubator, based on triplicate wells per time point. The average number of viable cells was counted on a hemacytochamber in the presence of trypan blue dye. The doubling time of the cell population was calculated from the exponential growth phase of the growth curve.

Induction of tumor formation. To determine the tumorigenicity of SNUOT-Rb1 cells *in vivo*, 1x10⁷ cells were suspended in

PBS and injected into the intravitreal cavity of BALB/c-nude mice. The SNUOT-Rb1-injected animals were checked for tumors over 4 weeks.

Microarray comparative genomic hybridization (CGH) analysis. Microarray CGH was performed using the Geno-Sensor Array 300 system, following the manufacturer's instructions (ABBOT-Vysis, Downers Grove, IL, USA). Each array contains 861 spots, representing 287 chromosomal regions that are commonly altered in human cancer. Briefly, 100 ng of genomic DNA were labeled by a random primer reaction during 2 h. Tumor DNA was labeled with Cy3 and the normal male reference DNA with Cy5. After the labeling reaction, the probes were digested with DNase at 15°C for 1 h, followed by two ethanol-purifications; finally the probe size was checked by gel electrophoresis. The hybridization mixture consisted of 2.5 μl of each of the differentially labeled DNAs plus 25 μl of hybridization buffer provided in the kit. This mixture was denatured at 80°C for 10 min, followed by incubation at 37°C for 1 h. Of this probe, 5 μl was applied onto the spotted area of the array under a coverslip and hybridized in a humid chamber containing 50% formamide (FA)/2X SSC at 37°C for 72 h. After hybridization, the arrays were washed 3 times in 50% FA/2X SSC at 40°C for 10 min/wash, followed by four 5-min washes in 1X SSC at room temperature. Finally, the arrays were briefly rinsed in distilled water, mounted and counterstained in the dark for 45 min with DAPI (4,6-diamino-2-phenylindole).

Array analysis was performed immediately after counterstaining using the GenoSensor scanner and software. Since each spot in the array is present in triplicates, the median of the three spots of each probe in the array was calculated and its log₂ transformed value was used for further analysis. A fluorescence ratio >1.25 (log₂, 0.32) was considered as a DNA gain, while DNA losses were scored when the ratio was <0.75 (log₂, -0.41).

Results

Pathological features of the primary tumor and isolation of SNUOT-Rb1. An eye with retinoblastoma was enucleated from a 3-year-old Korean child. As shown in hematoxylin/eosin staining, the endophytic retinoblastoma occupied over half of the vitreous cavity with some intravitreal seedings, but without invasion to the choroid or optic nerve head. The retina was shown to be extensively infiltrated by small, round cells with scanty cytoplasm and hyperchromatic nuclei. Viable tumor cells with mitotic features around blood vessels were surrounded by large area of necrosis, which were dispersed all over the tumor. There were small Flexner-Wintersteiner rosettes. (Fig. 1A) SNUOT-Rb1 was generated *in vitro* directly from cells isolated from fresh sterile retinoblastoma. SNUOT-Rb1 showed the microscopic features of fibroblast- or ganglion-like cells with adherent growth in a monolayer (Fig. 1B). The adherent growth is a unique characteristic of SNUOT-Rb1, different from other retinoblastoma cell lines such as Y79, or WERI-Rb1. RA triggered the differentiation of SNUOT-Rb1 to extend neuritis (Fig. 1B).

Morphological and growth characteristics of SNUOT-Rb1. As previously reported (10), RA upregulated retinoic acid

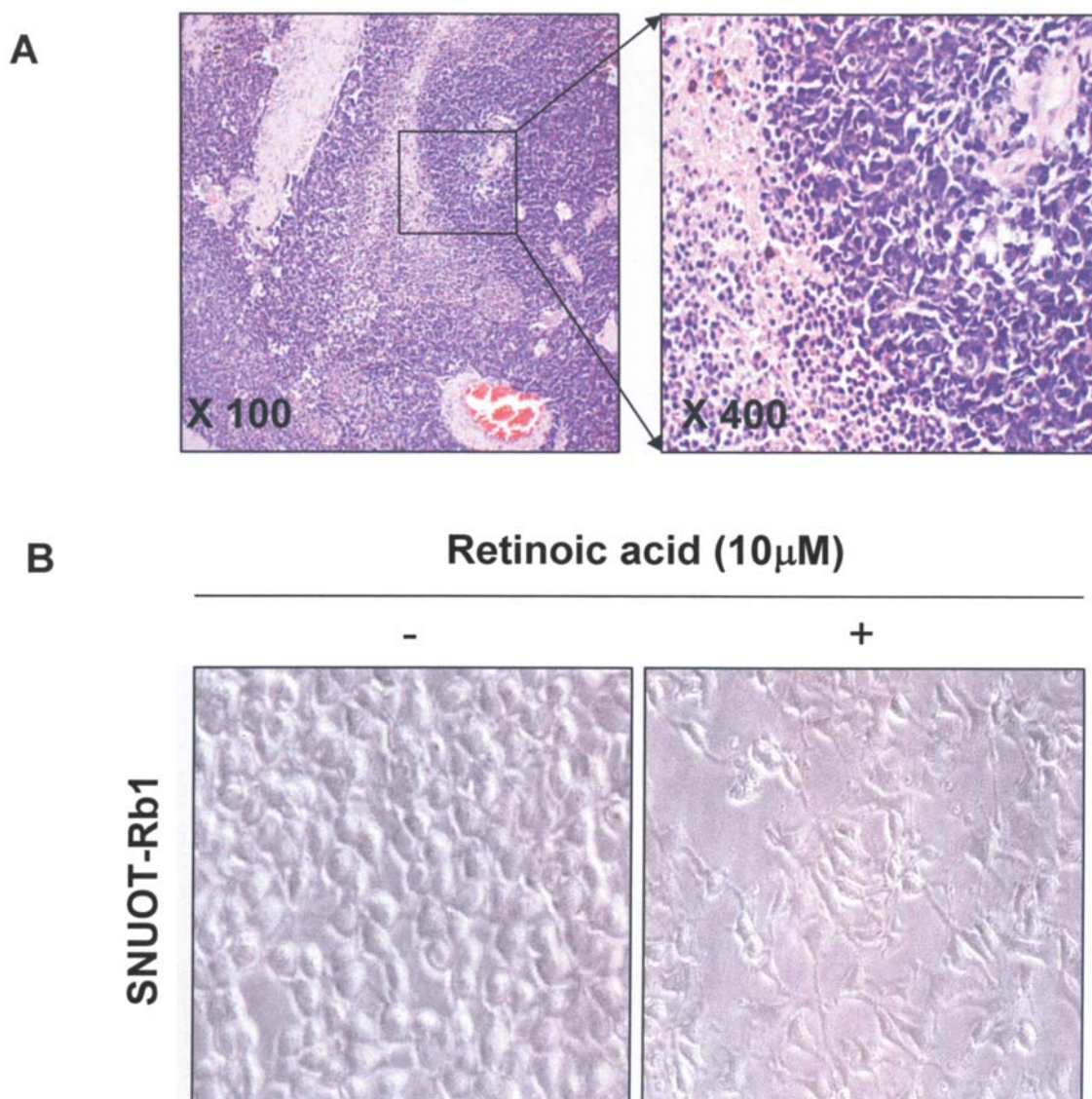


Figure 1. Histopathological features of the primary tumor and morphology of SNUOT-Rb1. Paraffin-embedded section of retinoblastoma tissue was stained with hematoxylin and eosin (A). SNUOT-Rb1 was isolated and then treated with 10 μ M RA for 10 days (B).

receptor α (RAR α) mRNA expression in both Y79 cells and SNUOT-Rb1 (Fig. 2A). Furthermore, the expression of GFAP and NSE were also detected through immunocytochemical staining (Fig. 2B) (11-13). The average population-doubling time of SNUOT-Rb1 was 24 h, whereas that of Y79 was 33 h in suspension or 50 h in attached monolayer (Fig. 2C) (8,9).

Tumor formation in vivo. Tumor formation was observed in all 30 nude mice intravitreally inoculated with 10^7 cells of SNUOT-Rb1. Tumor development was checked by indirect ophthalmoscopic examination. All tumors reached maximum size between 15 and 20 days after intravitreal inoculation. Twenty-one days after inoculation, nude mice were sacrificed and enucleated for pathological examination (20 eyes) and tumor cell reculture (10 eyes). The tumors were composed of small, round cells with scanty cytoplasm and hyperchromatic nuclei surrounded by large areas of necrosis. Their appearance was identical to the primary tumor (Fig. 3A). The tumor cells were isolated and recultured in adherent

growth, appearing morphologically identical to the SNUOT-Rb1 (Fig. 3B).

Cytogenetic analysis by CGH. We performed high-resolution matrix-CGH analysis on SNUOT-Rb1 and Y79. The chromosomal imbalances of Y79 were similar to those previously identified (14). SNUOT-Rb1 has significant chromosomal imbalances on chromosome 3, 9, 10, 11, 14, 16, 17, and 22. Comparing SNUOT-Rb1 to Y79, no significant chromosomal aberration was present on well-known sites of gene amplification in Y79, both the short arm of chromosome 2 and the long arm of chromosome 18 (Table I). N-myc amplification was not observed in SNUOT-Rb1. The significantly imbalanced chromosomal regions detected in SNUOT-Rb1 are listed in Table IB.

Discussion

The novel human retinoblastoma cell line, SNUOT-Rb1, was established from a 3-year old patient, who was diagnosed

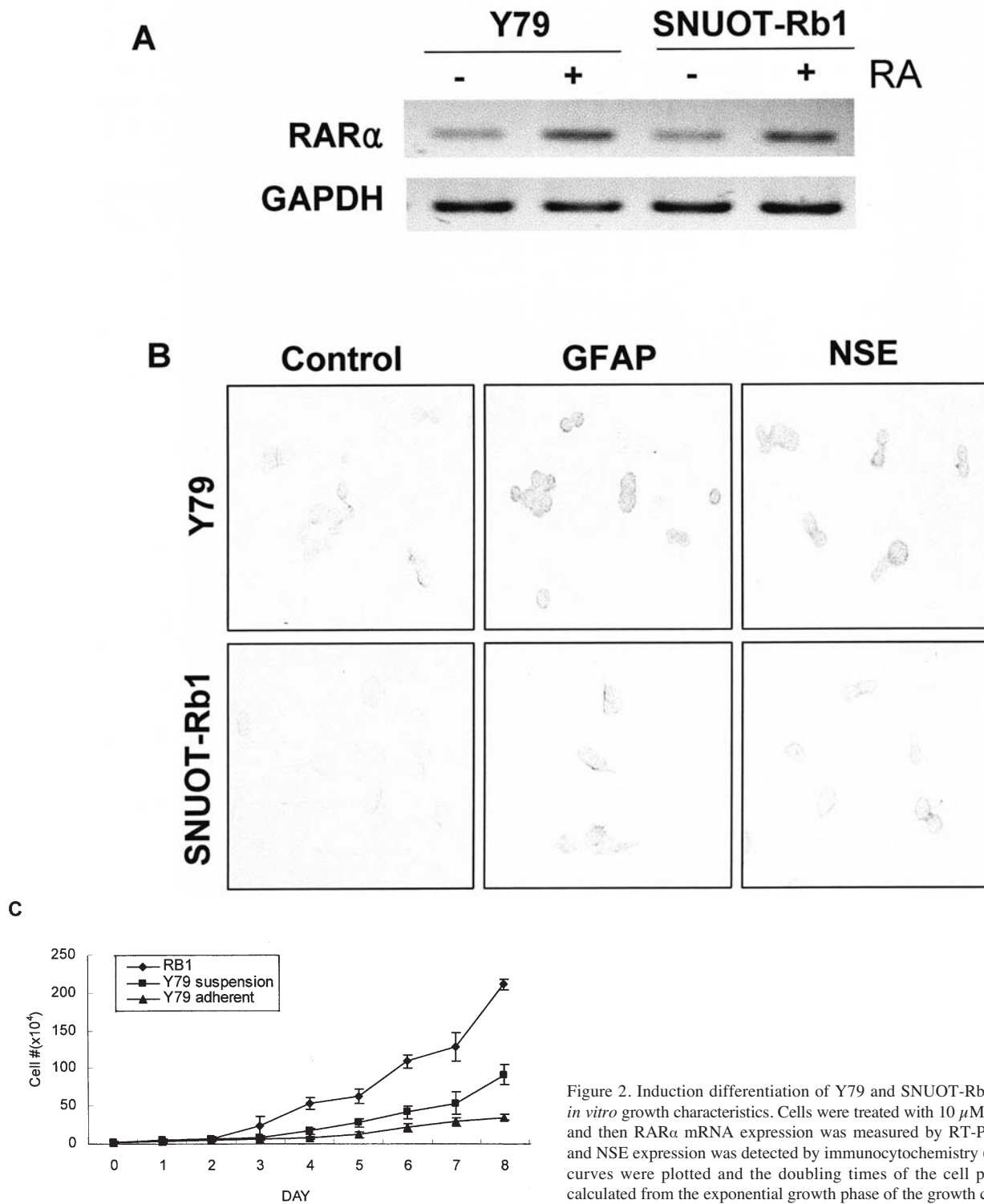


Figure 2. Induction differentiation of Y79 and SNUOT-Rb1 cell lines and *in vitro* growth characteristics. Cells were treated with 10 μ M RA for 10 days and then RAR α mRNA expression was measured by RT-PCR (A), GFAP and NSE expression was detected by immunocytochemistry (B). The growth curves were plotted and the doubling times of the cell population were calculated from the exponential growth phase of the growth curves (C).

as having a primary retinoblastoma at Seoul National University Children's Hospital. The malignancy of this cell line was determined by measuring the doubling time of cells and *in vivo* tumorigenesis. The doubling time of SNUOT-Rb1 is shorter than Y79 in adherent or floating growth, which means active proliferation of SNUOT-Rb1 and reconfirmed *in vivo* tumorigenesis maximal growth between 15 to 20 days. SNUOT-Rb1 has morphological and biochemical characteristics common to previous human retinoblastoma cell lines: morphological features of fibroblast- or ganglion-

like cells, and biochemical features of expression of GFAP and NSE (11-13). Furthermore, morphological and biochemical characteristics of SNUOT-Rb1 were constantly maintained in tumor cells isolated from tumors inoculated in the vitreal cavity of nude mice. In the present study, SNUOT-Rb1 was injected into the vitreal cavity of nude mice to examine tumor formation. This orthotopic implantation model mimics the pattern of local growth of retinoblastoma and may be an ideal model for determining the malignant potential of retinoblastoma cells (15).

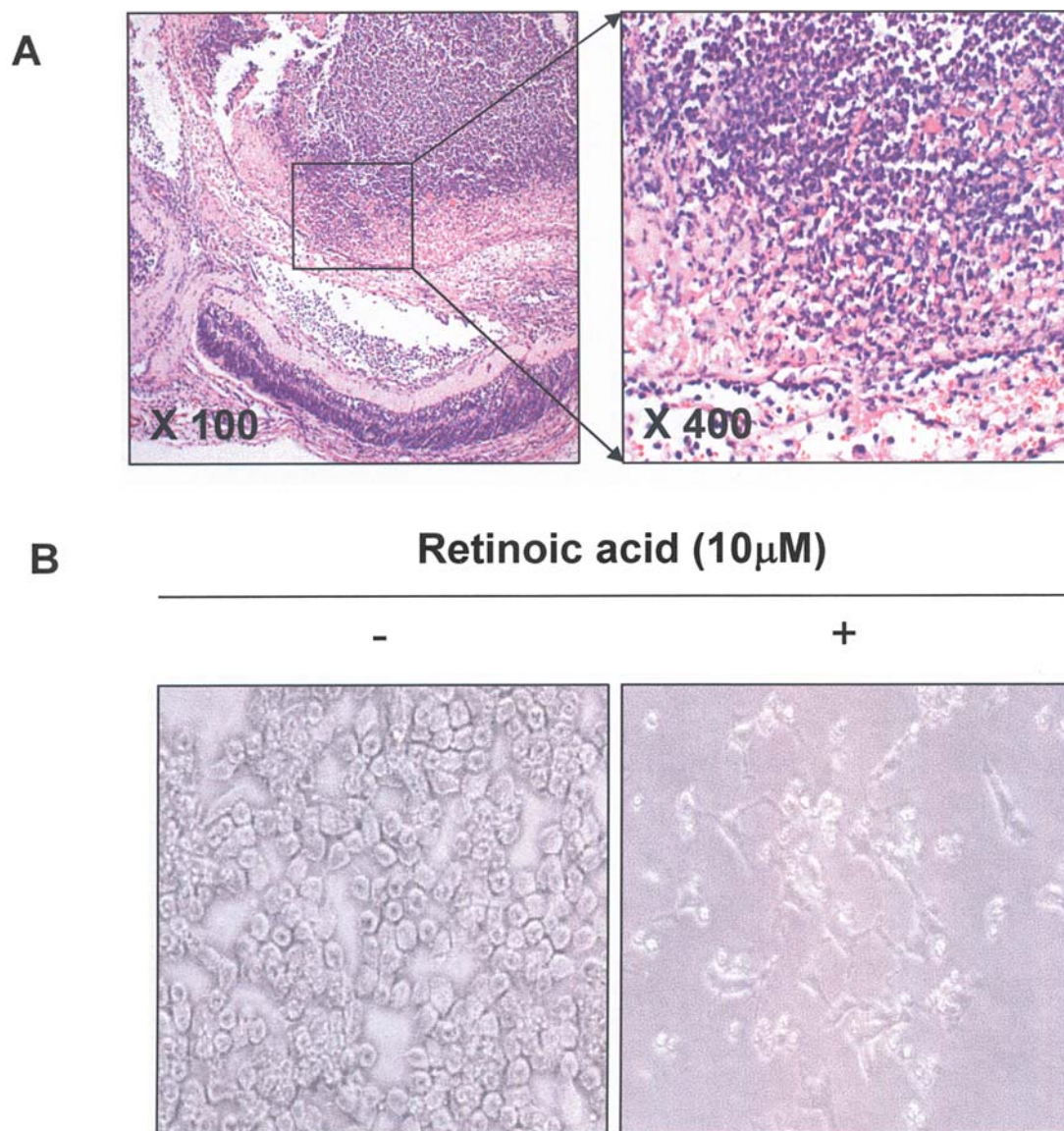


Figure 3. Analysis of tumorigenic potential of SNUOT-Rb1 in nude mice. SNUOT-Rb1 cells were injected into nude mice and the grown tumor was stained with hematoxylin and eosin (A). Tumor cells isolated from tumor tissue were treated with 10 μ M RA for 10 days (B).

Compared to Y79 or WERI-Rb1, SNUOT-Rb1 has an interesting, unique characteristic of growing in adherence, which is a great advantage over Y79 or WERI-Rb1 regarding easy manipulation for cell biologists to control gene expression. Therefore, even without cumbersome and sometimes expensive modifications to equipment, SNUOT-Rb1 may be suitable for use in a number of extremely important applications, including high-throughput drug screening formats, growth and expansion in roller bottles and expression cloning experiments.

In CGH, we found that SNUOT-Rb1 has significant chromosomal imbalances on chromosome 3, 9, 10, 11, 14, 16, 17, and 22. Chromosomal imbalances of SNUOT-Rb1 were not identical to those of Y79 (14). The genetic composition and aberration of an established cell line may differ from the aberrant cell from which it originated. N-myc amplification was not detected on SNUOT-Rb1, which could be an important prognostic factor presenting the proliferation activity of retinoblastoma cells. N-myc amplification could be a unique chromosomal aberration of Y79, whereas, n-myc amplification

might not be common to retinoblastoma in general (14). CGH analysis of SNUOT-Rb1 identified a minimal 16q genomic loss that was previously described for primary retinoblastoma tumors (16). Loss at 16q23.2 and 16q24.2 was present in SNUOT-Rb1. This chromosomal loss of 16q may implicate the cadherin-11 gene or the cadherin-13 gene as a potential tumor suppressor gene in retinoblastoma (17), but a cluster of cadherin genes is located at 16q22. Detection of chromosomal loss by CGH has a resolution of \sim 10 to 20 Mbp (18). Further studies for chromosomal aberrations of SNUOT-Rb1 remain necessary using retinoblastoma tumors.

In conclusion, SNUOT-Rb1 is a novel human retinoblastoma cell line, which has unique characteristics of adherent growth and chromosomal imbalances different from Y79 or WERI-RB1. Therefore, SNUOT-Rb1 should have many advantages for the study of biological and genetic characteristics. Also, an orthotopic implantation model using SNUOT-Rb1 might be the most representative of retinoblastoma formation in the retina.

Table I. CGH analysis: genomic imbalances detected by CGH in Y79 (A) and SNUOT-Rb1 (B).

Chromosome no.	Locus name	Cytogenetic location	Mean ratio	Non-modal (p<x)	Gain/loss
A					
1	LAMC2	1q25-q31	1.35	0.0001	++
1	TGFB2	1q41	1.34	0.0002	++
1	WI-5663, WI-13414	1q21	1.28	0.0005	++
1	AKT3	1q44	1.30	0.001	++
1	PTGS2 (COX2)	1q31.1	1.23	0.005	++
1	1QTEL10	1q tel	1.21	0.01	++
2	MYCN (n-myc)	2p24.1	19.65	0.0001	++
2	MSH2, KCNK12	2p22.3-2p22.1	1.38	0.0001	++
2	GNLY	2p12-q11	1.47	0.0001	++
2	REL	2p13-p12	1.33	0.0005	++
5	DHFR, MSH3	5q11.2-q13.2	1.21	0.01	++
6	PIM1	6p21.2	1.39	0.0001	++
6	6PTEL48	6p tel	1.27	0.001	++
6	CCND3	6p21	1.24	0.005	++
8	E2F5	8p22-q21.3	1.19	0.01	++
15	MAP2K5	15q23	1.40	0.0001	++
16	CYLD	16q12-q13	0.56	0.0001	--
17	NME1 (NME23)	17q21.3	1.49	0.0001	++
17	RPS6KB1 (STK14A)	17q23	1.46	0.0001	++
17	D17S1670	17q23	1.52	0.0001	++
17	TK1	17q23.2-q25.3	1.56	0.0001	++
17	AFM217YD10	17q tel	1.56	0.0001	++
17	TP53 (p53)	17p13.1	1.32	0.0002	++
17	SHGC-103396	17q tel	1.35	0.0002	++
17	NF1 3'	17q11.2	1.24	0.005	++
17	BRCA1	17q21	1.24	0.005	++
17	ERBB2 (HER-2)	17q11.2-17q12	1.26	0.005	++
17	PPARBP (PBP)	17q12	1.26	0.01	++
18	SHGC17327	18p tel	1.71	0.0001	++
18	YES1	18p11.31-p11.21	1.46	0.0001	++
18	TYMS (TS)	18p11.32	1.48	0.0001	++
18	LAMA3	18q11.2	1.56	0.0001	++
18	FRA18A (D18S978)	18q12.3	1.41	0.0001	++
18	18QTEL11	18q tel	1.65	0.0001	++
18	D18S552	18p tel	1.31	0.0005	++
18	BCL2 3'	18q21.3	1.29	0.002	++
20	20QTEL14	20q tel	0.62	0.0001	--
21	RUNX1 (AML1)	21q22.3	1.37	0.0001	++
21	DYRK1A	21q22	1.41	0.0001	++
21	21QTEL08	21q tel	1.47	0.0001	++
21	PCNT2 (KEN)	21q tel	1.28	0.001	++
21	D21S341, D21S342	21q22.3	1.25	0.01	++
X	OCRL1	Xq25	1.61	0.0001	++
B					
1	D1S214	1p36.31	1.35	0.01	++
1	D1S1635	1p36.22	1.33	0.01	++
1	D1S199	1p36.13	1.33	0.01	++
3	RASSF1	3p21.3	0.7	0.005	--

Table I. Continued.

Chromosome no.	Locus name	Cytogenetic location	Mean ratio	Non-modal (p<x)	Gain/loss
3	FHIT	3p14.2	0.70	0.005	--
3	p44S10	3p14.1	0.69	0.005	--
9	AF170276	9p tel	0.60	0.0001	--
9	D9S913	9p tel	0.44	0.0001	--
9	MTAP	9p21.3	0.56	0.0001	--
9	CDKN2A (P16), MTAP	9p21	0.52	0.0001	--
10	D10S167	10p11-10q11	0.71	0.005	--
10	GATA3	10p15	0.72	0.01	--
10	FGFR2	10q26	0.71	0.01	--
11	CCND1	11q13	1.59	0.0001	++
11	MLL	11q23	1.77	0.0001	++
11	GARP	11q13.5-q14	1.59	0.0002	++
11	EMS1	11q13	1.52	0.0005	++
11	PAK1	11q13-q14	1.57	0.0005	++
11	RDX	11q22.3	1.51	0.0005	++
11	INS	11p tel	0.64	0.001	--
11	CDKN1C (p57)	11p15.5	0.65	0.001	--
11	FGF4, FGF3	11q13	1.48	0.001	++
11	ATM	11q22.3	1.43	0.002	++
11	WT1	11p13	0.71	0.005	--
11	KAL1	11p11.2	0.69	0.005	--
14	AKT1	14q32.32	0.69	0.005	--
14	TCL1A	14q32.1	0.70	0.01	--
16	ABCC1 (MRP1)	16p13.1	0.56	0.0001	--
16	stSG30213	16q tel	0.64	0.0002	--
16	16QTEL013	16q tel	0.66	0.001	--
16	CDH13	16q24.2-q24.3	0.67	0.002	--
16	EMP2	16p13.3	0.70	0.005	--
16	LZ16	16q24.2	0.71	0.005	--
16	CYLD	16q12-q13	0.72	0.01	--
16	FRA16D	16q23.2	0.72	0.01	--
17	LLGL1	17p12-17p11.2	0.66	0.001	--
17	282M15/SP6	17p tel	0.66	0.002	--
17	FLI, TOP3A	17p12-17p11.2	0.69	0.002	--
17	W1-14673	17p tel	0.72	0.01	--
19	129F16/SP6	19p tel	0.71	0.01	--
19	CCNE1	19q12	0.73	0.01	--
22	BCR	22q11.23	0.63	0.0005	--
22	TBX1	22q11.23	0.72	0.005	--
22	GSCL	22q11.21	0.72	0.01	--

Acknowledgements

Thanks go to Digital Genomics Ltd. (Seoul, South Korea) for microarray-CGH analysis and Hyun Suk Jeong and Su Hee Jeong for technical help of experiments. This study was supported by a grant from the National R&D program for cancer control, Ministry of Health and Welfare, Republic of Korea (05-20240-1).

References

1. Newsham IF, Hadjistilianou T and Cavenee WK: Retinoblastoma. In: The Genetic Basis of Human Cancer. 2nd edit. Vogelstein B and Kinzler KW (eds). McGraw-Hill, New York, pp357-386, 2002.
2. Gallie BL and Phillips RA: Retinoblastoma: a model of oncogenesis. *Ophthalmology* 91: 666-672, 1984.
3. Conway RM, Wheeler SM, Murray TG, Jockovich ME and O'Brien JM: Retinoblastoma: animal models. *Ophthalmol Clin North Am* 18: 25-39, 2005.

4. Godbout R, Dryja TP, Squire JA, Gallie BL and Phillips RA: Somatic inactivation of genes on chromosome 13 is a common event in retinoblastoma. *Nature* 304: 451-453, 1983.
5. Gallie BL, Campbell C, Devlin H, Duckett A and Squire JA: Developmental basis of retinal-specific induction of cancer by RB mutation. *Cancer Res* 59: 1731-1735, 1999.
6. Lee EY, Chang CY, Hu N, *et al.*: Mice deficient for Rb are nonviable and show defects in neurogenesis and hematopoiesis. *Nature* 359: 284-288, 1992.
7. Horsthemke B: Genetics and cytogenetics of retinoblastoma. *Cancer Genet Cytogenet* 63: 1-7, 1992.
8. Reid TW, Albert DM, Rabson AS, *et al.*: Characteristics of an established cell line of retinoblastoma. *J Natl Cancer Inst* 53: 347-360, 1974.
9. McFall RC, Sery TW and Makadon M: Characterization of a new continuous cell line derived from a human retinoblastoma. *Cancer Res* 37: 1003-1010, 1977.
10. Li A, Zhu X and Craft CM: Retinoic acid upregulates cone arrestin expression in retinoblastoma cells through a cis element in the distal promoter region. *Invest Ophthalmol Vis Sci* 43: 1375-1383, 2002.
11. Messmer EP, Font RL, Kirkpatrick JB and Hopping W: Immunohistochemical demonstration of neuronal and astrocytic differentiation in retinoblastoma. *Ophthalmology* 92: 167-173, 1985.
12. Xu KP, Liu SL and Ni C: Immunohistochemical evidence of neuronal and glial differentiation in retinoblastoma. *Br J Ophthalmol* 79: 771-776, 1995.
13. Perentes E, Herbort CP, Rubinstein LJ, *et al.*: Immunohistochemical characterization of human retinoblastomas *in situ* with multiple markers. *Am J Ophthalmol* 103: 647-658, 1987.
14. Bie W, Squire JA, Fraser M, Paterson MC and Godbout R: Mitochondrial ATP synthase α -subunit gene amplified in a retinoblastoma cell line maps to chromosome 18. *Genes Chromosomes Cancer* 14: 63-67, 1995.
15. Chevez-Barrios P, Hurwitz MY, Louie K, *et al.*: Metastatic and nonmetastatic models of retinoblastoma. *Am J Pathol* 157: 1405-1412, 2000.
16. Chen D, Gallie BL and Squire JA: Minimal regions of chromosomal imbalance in retinoblastoma detected by comparative genomic hybridization. *Cancer Genet Cytogenet* 129: 57-63, 2001.
17. Marchong MN, Chen D, Corson TW, *et al.*: Minimal 16q genomic loss implicates cadherin-11 in retinoblastoma. *Mol Cancer Res* 2: 495-503, 2004.
18. Kallioniemi A, Kallioniemi OP, Sudar D, *et al.*: Comparative genomic hybridization for molecular cytogenetic analysis of solid tumors. *Science* 258: 818-821, 1992.